Evans function and blow-up methods in critical eigenvalue problems

Björn Sandstede
Department of Mathematics
The Ohio State University
Columbus, OH 43210, USA

Arnd Scheel
Department of Mathematics
University of Minnesota
Minneapolis, MN 55455, USA

March 26, 2003

Abstract

Contact defects are one of several types of defects that arise generically in oscillatory media modelled by reaction-diffusion systems. An interesting property of these defects is that the asymptotic spatial wavenumber is approached only with algebraic order $O(1/x)$ (the associated phase diverges logarithmically). The essential spectrum of the PDE linearization about a contact defect always has a branch point at the origin. We show that the Evans function can be extended across this branch point and discuss the smoothness properties of the extension. The construction utilizes blow-up techniques and is quite general in nature. We also comment on known relations between roots of the Evans function and the temporal asymptotics of Green's functions, and discuss applications to algebraically decaying solitons.

1 Introduction

The goal of this paper is to investigate the stability properties of certain nonlinear waves that arise in dissipative, pattern-forming partial differential equations (PDEs). Consider a reaction-diffusion system

$$U_t = DU_{xx} + F(U), \tag{1.1}$$

posed on the real line $x \in \mathbb{R}$, where $U \in \mathbb{R}^N$ and D is a diagonal positive diffusion matrix. We assume that (1.1) supports a family of wave-train solutions $U(x,t) = U_{\rm wt}(kx - \omega t; k)$ that are 2π-periodic in $\phi = kx - \omega t$. Wave trains arise typically as one-parameter families for which the non-zero temporal frequency ω and the non-zero spatial wavenumber k are related through a nonlinear dispersion relation $\omega = \omega_{\rm nl}(k)$. Thus, the wave train with wavenumber k travels with phase speed $c_{\rm p} = \omega_{\rm nl}(k)/k$. Of importance is also the group velocity $c_{\rm g} = \omega'_{\rm nl}(k)$ which can be thought of as the speed with which small initial perturbations are transported along spectrally stable wave trains.

We are interested in *defects* which are solutions to (1.1) that are time periodic in an appropriate moving coordinate frame and that converge to two, possibly different, wave trains as $x \to \pm\infty$. See Figure 1 for an illustration. In an accompanying paper [21], we give a list of four defects, namely sinks, sources, contact defects and transmission defects, that occur generically in such a

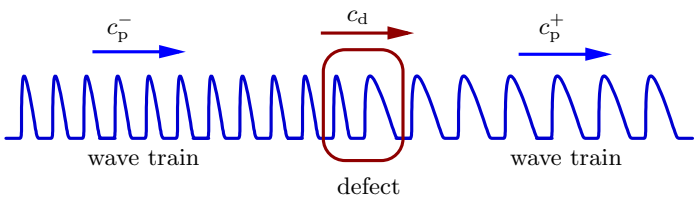

Figure 1: *A defect that travels with speed $c_{\rm d}$ through wave trains which themselves travel with phase velocities $c_{\rm p}^-$ behind and $c_{\rm p}^+$ ahead of the defect.*

medium. The characteristics that distinguish these four defect types are the group velocities $c_{\rm g}^\pm$ of the asymptotic wave trains at $x = \pm\infty$, measured relative to the speed of the defect $c_{\rm d}$: Sinks are shock-like structures for which $c_{\rm g}^- > c_{\rm d} > c_{\rm g}^+$ so that perturbations are transported towards the defect. Transmission defects are characterized by $c_{\rm g}^\pm > c_{\rm d}$ or $c_{\rm g}^\pm < c_{\rm d}$ so that the characteristic curves enter at one side and leave at the other side of the defect. Sources generate waves for they satisfy $c_{\rm g}^- < c_{\rm d} < c_{\rm g}^+$ so that perturbations travel away from the defect. In this paper, we focus on *contact defects* that are asymptotic at $x = \pm\infty$ to the same wave train and that travel with the group velocity $c_{\rm d} = c_{\rm g}$ of the asymptotic wave train. These defect are referred to as *contact discontinuities*, see for instance [22], in the context of conservation laws from which we borrowed the terminology.

Contact defects occur in one-parameter families that are parametrized by the wavenumber k of the asymptotic wave train. We seek them as solutions $U(x,t) = U_{\rm d}(x - c_{\rm g}t, \omega_{\rm d}t)$ of (1.1) that satisfy

$$\begin{aligned} U_{\rm d}(x - c_{\rm g}t, \omega_{\rm d}t) &= U_{\rm d}(x - c_{\rm g}t, \omega_{\rm d}t + 2\pi) \qquad (x,t) \in \mathbb{R} \times \mathbb{R}^+ \\ |U_{\rm d}(x - c_{\rm g}t, \omega_{\rm d}t) - U_{\rm wt}(kx - \omega_{\rm nl}(k)t - \theta_\pm(x - c_{\rm g}t); k)| &\to 0 \qquad \text{for } x \to \pm\infty \end{aligned}$$

where we assume that $\omega_{\rm d} := \omega_{\rm nl}(k) - c_{\rm g}k \neq 0$ (this assumption simply means that the group and phase velocities of the selected wave train $U_{\rm wt}(kx - \omega_{\rm nl}(k)t; k)$ do not coincide). As we will show in Section 3.1, a characteristic common feature of contact defects is the algebraic relaxation of the wavenumber $\theta'_\pm(x) = {\rm O}(1/|x|)$ for $|x \to \infty$ together with the logarithmic divergence of the asymptotic phase $\theta_\pm(x)$. The reason for the algebraic decay is, roughly speaking, that the asymptotic wave train is in a saddle-node bifurcation configuration when considered in a frame that moves with its group velocity. At saddle-nodes, however, spatial convergence is only algebraic and not exponential.

Contact defects have been observed experimentally in several different contexts (see [21] for details). One example are line defects that occur at period-doubling bifurcations of spiral waves [23]. We refer to Figure 2 for the results of numerical simulations in the Rössler model with diffusion.

Our goal is to obtain a proper description of the reaction-diffusion system, linearized about a contact defect, and of the spectrum of the associated linear period map; recall that defects are time-periodic solutions of (1.1), considered in an appropriate co-moving frame. The key issue is to trace eigenvalues of the linearized period map into the essential spectrum by using a variant of the Evans function that was originally introduced in [1]. The main obstacle is the simultaneous presence of a branch point in the continuous spectrum and the weak algebraic decay of the x-dependent coefficients in the linearized equation that appear since the profile of the contact defect depends on

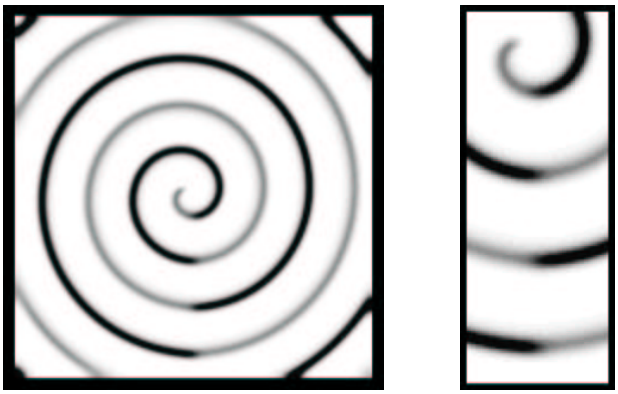

Figure 2: *The left picture shows a contour plot of a planar spiral wave that arises after the asymptotic wave trains went through a period-doubling bifurcation. To accommodate the geometry, a contact defect forms along a straight line (a magnification of the defect is shown in the right plot).*

x. We believe that a proper understanding of the linearized problem will prove useful in future work on nonlinear stability and interaction properties of contact defects. Furthermore, the techniques that we develop here enable us to assign linear stability properties in nonlinear bifurcation diagrams such as those arising in locking and unlocking bifurcations of different types of defects [21]. We remark that it was shown in [18], see also [12], that the Evans function can be constructed for algebraically decaying coefficients as long as one stays away from the absolute spectrum that was introduced in [19]. Note also that, thanks to the Gap Lemma [8, 11], exponentially decaying waves are much easier to handle. In that sense, the results given here can be interpreted as extending the Evans function beyond the Gap Lemma. We mention the related work [17], which came out after our manuscript was submitted, where the Evans function is considered for certain 2×2 Lax operators with algebraically decaying potentials.

The eigenvalue problems that we consider are critical in the sense that the inhomogeneity $\mathrm{O}(1/x)$ in the coefficients scales in the same way as the leading differential operator. Our methods apply more generally to eigenvalue problems which are essentially one-dimensional and respect this characteristic type of scaling. We view the eigenvalue and the existence problem simultaneously as a dynamical system in the spatial variable x. On an appropriate center manifold, the critical scaling behavior is reflected in a scaling invariance of the leading term of the Taylor jet. We exploit this scaling invariance by using invariant coordinates which allow us to remove the degeneracy in the linearization in the form of an Euler multiplier of the differential equations. The entire procedure is motivated by the geometric approach to singularly perturbed problems via blow-up techniques that were developed by Dumortier [5] and that have also been used more recently by Szmolyan and coworkers [6, 14]. We also mention recent work by Howard [9, 10] who obtained related results on degenerate shock waves using different methods.

In the blow-up coordinates that we use here, the influence of the far field becomes geometrically separated from the influence of the spatial inhomogeneity. Whereas the far field contributes a $\sqrt{\lambda}$ branch point singularity to the Evans function as in eigenvalue problems with exponential spatial

decay, the inhomogeneities introduce $\sqrt{\lambda}\log\lambda$-terms in the expansion for the Evans function near the origin via resonant terms in the Dulac map near a 1:1-resonant hyperbolic equilibrium.

In the particular case of a contact defect, we derive an expansion for the Evans function of the form

$$\mathcal{E}(\gamma) = \gamma\,\mathcal{E}_0(\gamma, \gamma\log\gamma), \qquad \gamma = \sqrt{\lambda}$$

where $\mathcal{E}_0(\gamma,\eta)$ is of class C^∞ in a neighborhood of the origin with a cut along the absolute spectrum (see [19] for the definition of the absolute spectrum and its relevance in large but finite domains). The construction allows us to compute Taylor jets of $\mathcal{E}$, and we show that typically $\partial_\eta\mathcal{E}_0(0,0) \neq 0$. In particular, the Evans function is not analytic in $\gamma = \sqrt{\lambda}$ in contrast to the case of exponentially decaying waves [8, 11].

The simplest example for critical inhomogeneous coefficients arises in eigenvalue problems for the Laplacian with radial symmetry. Indeed, the $1/r$-curvature terms in the eigenvalue problem

$$u_{rr} + \frac{n-1}{r}u_r = \lambda u \tag{1.2}$$

obey the same critical scaling behavior as the one described above. Although "everything" is known about the eigenvalue problem (1.2), we revisit it in Section 2 to illustrate the methods and phenomena that we shall encounter again in Section 3, where we carry out the actual blow-up of the eigenvalue problem for contact defects.

Our main results are Theorems 1–3 that can be found in Sections 3.1, 3.6 and 3.7. In Section 4, we discuss a variety of applications of these techniques to other limiting cases of the Evans-function approach such as to the boundary of the region where the Gap Lemma applies and to eigenvalue problems for algebraically decaying solitons.

2 The radial Laplacian and the Evans function

Consider the eigenvalue problem (1.2)

$$u'' + \frac{n-1}{r}u' = \lambda u, \qquad ' = \frac{\mathrm{d}}{\mathrm{d}r}. \tag{2.1}$$

We seek solutions so that $u(r)$ and $u'(r)$ are bounded as $r \to 0$ and as $r \to \infty$. For $n = 1$, we use Neumann boundary conditions at $r = 0$. The operator on the left-hand side of (2.1) is closed and densely defined for instance on the space $C^0_{\mathrm{unif}}(\mathbb{R}^+)$ of bounded and uniformly continuous functions and also on $L^p(\mathbb{R}^+)$ equipped with the weighted measure $r^{n-1}\mathrm{d}r$ induced by the Lebesgue measure on $\mathbb{R}^n$. We emphasize that the arguments presented below for (2.1) generalize easily to equations with an additional algebraically localized potential $V(r)u$ or gradients $W(r)u_r$.

We rewrite (2.1) as a first-order differential equation

$$\begin{aligned} u' &= v \\ v' &= -\frac{n-1}{r}v + \lambda u. \end{aligned} \tag{2.2}$$

Note that each bounded solution has an expansion $u(r) = u_0 + \mathrm{O}(r^2)$ and $v(r) = \mathrm{O}(r)$ at $r = 0$. If we use the homogeneous coordinates $z = v/u$ in the projective space, write $\lambda = \gamma^2$, and introduce $\kappa = 1/r$ as a new dependent variable, we obtain

$$\begin{aligned} z' &= -(n-1)\kappa z + \gamma^2 - z^2 \\ \kappa' &= -\kappa^2 \\ \gamma' &= 0. \end{aligned} \tag{2.3}$$

We remark that u and v can be recovered easily once z is known. For the sake of clarity, we restrict ourselves in this section to real values of γ.

The equation in projective space is homogeneous of degree 2. We therefore introduce blow-up coordinates and replace $(z, \kappa, \gamma) \in \mathbb{R}^3$ by polar coordinates on $\mathbb{R}_+ \times S^2$, thus blowing up the origin in $\mathbb{R}^3$ to a two-sphere $\{0\} \times S^2$. On the two-sphere, we choose two different sets of homogeneous coordinates. The *singular chart* given by

$$z_1 = \frac{z}{\kappa}, \qquad \gamma_1 = \frac{\gamma}{\kappa}, \qquad \kappa_1 = \kappa$$

regularizes the critical decay in the inhomogeneity, whereas the *rescaling chart*, defined via

$$z_2 = \frac{z}{\gamma}, \qquad \kappa_2 = \frac{\kappa}{\gamma}, \qquad \gamma_2 = \gamma,$$

takes care of the singularity at $\gamma = 0$. In the singular chart, the equations become

$$\begin{aligned} z_1' &= \kappa_1 \left[\gamma_1^2 - (n-2)z_1 - z_1^2\right] \\ \gamma_1' &= \kappa_1 \left[\gamma_1\right] \\ \kappa_1' &= \kappa_1 \left[-\kappa_1\right], \end{aligned}$$

while we obtain

$$\begin{aligned} z_2' &= \gamma_2 \left[1 - (n-1)\kappa_2 z_2 - z_2^2\right] \\ \kappa_2' &= \gamma_2 \left[-\kappa_2^2\right], \\ \gamma_2' &= 0 \end{aligned}$$

in the rescaling chart. In both charts, the equation has an Euler multiplier given by κ_1 in the singular chart and by γ_2 in the rescaling chart. We can therefore rescale r by defining the new independent variable $\mathrm{d}\rho = \kappa_1 \mathrm{d}r$ in the singular chart and $\mathrm{d}\rho = \gamma_2 \mathrm{d}r$ in the rescaling chart. We begin by discussing the phase portrait in the rescaling chart. Writing $\dot{} = \mathrm{d}/\mathrm{d}\rho$ and omitting the trivial equation for γ, we obtain

$$\begin{aligned} \dot{z}_2 &= 1 - (n-1)\kappa_2 z_2 - z_2^2, \\ \dot{\kappa}_2 &= -\kappa_2^2. \end{aligned}$$

The phase portrait is shown in Figure 3. For $\gamma > 0$, the equilibrium $(z_2, \kappa_2, \gamma_2) = (-1, 0, \gamma)$ corresponds to the limit as $r \to \infty$ of the r-dependent stable subspace of solutions to (2.2) that

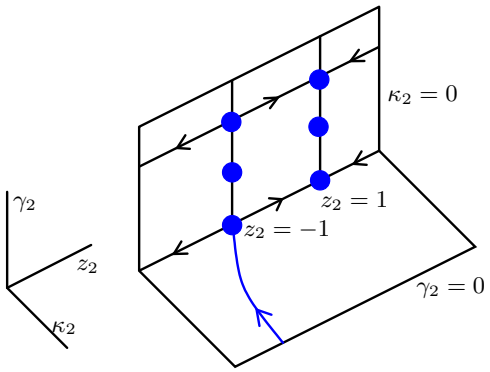

Figure 3: *The phase portrait in the rescaling chart for* $\gamma > 0$.

decay exponentially as $r \to \infty$. The center manifold of this equilibrium is unique in the half space $\kappa > 0$ and is, in fact, given by the set of solutions that converge to the equilibrium. Note, however, that the center manifold is not unique for $\kappa < 0$.

As a consequence of this discussion, the r-dependent stable subspace, i.e. the space of all solutions to (2.2) that converge to zero as $r \to \infty$, is, for $\gamma > 0$, given by the stable manifold of the equilibrium $(z_2, \kappa_2, \gamma_2) = (-1, 0, \gamma)$. Thus, to determine its fate as r becomes smaller, we have to follow the stable manifold backward in radial time, uniformly in $\gamma > 0$. Thus, we begin with the stable manifold at $\gamma_2 = 0$. Since $\dot{z}_2 = 1$ for $z_2 = 0$, we can conclude that the stable manifold is contained in the quadrant $z_2 < 0$, $\kappa_2 > 0$. A standard growth estimate shows that we can follow the solution backward in time until we reach $\kappa_2 = 1/\delta$, where $\delta > 0$ is arbitrarily small but fixed. At this point, we can switch to the singular chart which is regular at $\gamma = 0$ so that we can locate the stable manifold uniformly in γ near zero. Hence, we transform the point $(z_2, \kappa_2, \gamma_2) = (z_2^*, 1/\delta, \gamma)$ with $z_2^* < 0$ into the singular-chart coordinates which gives

$$z_1 = \frac{z}{\kappa} = \frac{z_2}{\kappa_2} = z_2^* \delta < 0, \qquad \gamma_1 = \frac{\gamma}{\kappa} = \frac{1}{\kappa_2} = \delta, \qquad \kappa_1 = \kappa = \frac{\gamma}{\delta}. \tag{2.4}$$

The next step is then to discuss the dynamics of the equation

$$\begin{aligned} \dot{z}_1 &= \gamma_1^2 - (n-2)z_1 - z_1^2 \\ \dot{\gamma}_1 &= \gamma_1 \\ \dot{\kappa}_1 &= -\kappa_1 \end{aligned}$$

in the singular chart. The phase portrait, shown in Figure 4, depends crucially on whether $1 \leq n < 2$, $n = 2$, or $n > 2$. Since we will encounter the case $n = 3$ in Section 3, we will focus on $n = 3$ and briefly comment on the other cases later.

Thus, upon setting $n = 3$, we obtain the equation

$$\begin{aligned} \dot{z}_1 &= \gamma_1^2 - z_1 - z_1^2 \\ \dot{\gamma}_1 &= \gamma_1 \\ \dot{\kappa}_1 &= -\kappa_1 \end{aligned} \tag{2.5}$$

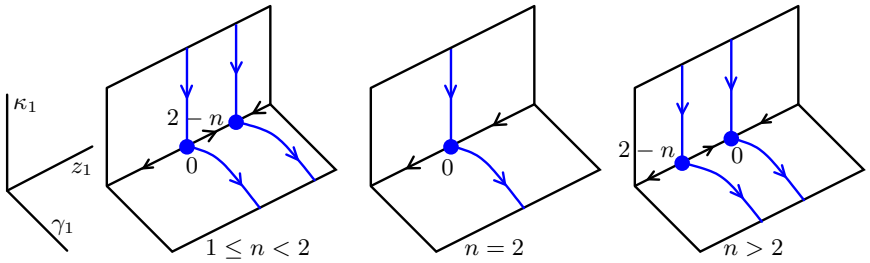

Figure 4: *The phase portraits in the singular chart for different dimensions n.*

in the singular chart. The planes $\gamma_1 = 0$ and $\kappa_1 = 0$ as well as their intersection, which is the z_1-axis, are flow invariant. Inside the plane $\kappa_1 = 0$, which corresponds to the singular limit $r = \infty$, the z_1-axis is attracting in backward radial time, and every trajectory in the quadrant $z_1 < 0$, $\gamma_1 > 0$ converges to the equilibrium $(z_1, \gamma_1) = (-1, 0)$ in backward time since the vector field is $\dot{z}_1 = \gamma_1^2 \geq 0$ at $z_1 = 0$. Note that the initial data $(z_1, \gamma_1, \kappa_1) = (z_2^* \delta, \delta, \gamma/\delta)$ in (2.4) lie in this quadrant for $\gamma = 0$. In particular, for $\gamma = 0$, there exists a singular heteroclinic orbit that connects $(z_1, \gamma_1) = (-1, 0)$ in the singular chart to $(z_2, \kappa_2) = (-1, 0)$ in the rescaling chart, see Figure 5. These arguments take care of the transition between the singular and the rescaling chart.

It remains to study the dynamics of (2.5) in the singular chart near the equilibrium $(z_1, \gamma_1) = (-1, 0)$. Observe that this equilibrium has a one-dimensional stable manifold which is given explicitly by the set $z_1 = -1$, $\gamma_1 = 0$ and $\kappa_1 > 0$. For $\gamma > 0$ small, solutions with initial conditions given by (2.4) will intersect a Poincaré section at $\kappa_1 = \delta$ close to the stable manifold of $(z_1, \gamma_1) = (-1, 0)$, see Figure 5. In particular, the subspace of all solutions to (2.2) that decay as $r \to \infty$ converges as $\gamma \to 0$ to the stable manifold of the equilibrium $(z_1, \gamma_1, \kappa_1) = (-1, 0, 0)$. Transforming back to the original coordinates, we see that this stable manifold is spanned precisely by all solutions to (2.2) with $1/r$-decay in the u-component at $r = \infty$.

We are now in a position to define an Evans function. We denote by $z_+ = z_1$ the γ-dependent z-component of the stable manifold of the equilibrium $(z_2, \kappa_2, \gamma_2) = (-1, 0, \gamma)$, evaluated in the singular chart at $\kappa_1 = 1$. The observations above show that $z_+(\gamma) \to -1$ as $\gamma \to 0$. Analogously, we denote by z_- the projective subspace, evaluated at radial time $r = 1$, that corresponds to solutions of (2.2) that remain bounded as $r \to 0$. Since this subspace depends analytically on λ, we have $z_- = \mathrm{O}(\gamma^2)$. We can now define an Evans function via

$$\mathcal{E}(\gamma) = z_-(\gamma) - z_+(\gamma) \tag{2.6}$$

so that zeros of $\mathcal{E}(\gamma)$ with $\gamma > 0$ correspond to eigenvalues $\lambda = \gamma^2$ of the operator on the left-hand side of (2.1). The discussion above shows that we have the expansion

$$\mathcal{E}(\gamma) = 1 + \mathrm{o}_\gamma(1)$$

for $n = 3$.

More generally, we have $z_-(\gamma) = \mathrm{O}(\gamma^2)$ for $n \geq 1$ since the only solution of (2.2) with $\lambda = 0$ that remains bounded as $r \to 0$ is the constant function; this function, however, corresponds to $z_1 = 0$.

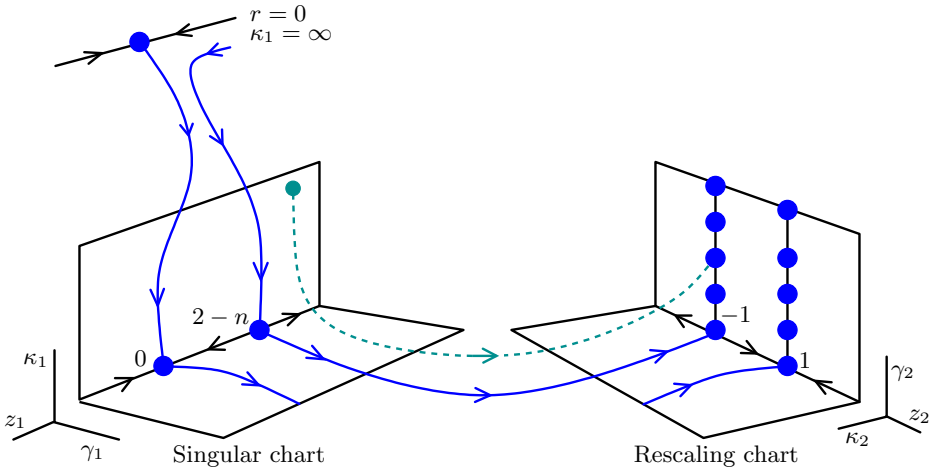

Figure 5: *The connecting orbits between $r = 0$ and the singular chart and from the singular to the rescaling chart for $n > 2$. The z_1-component $z_+(\gamma)$ of the left endpoint of the dashed line, which indicates the stable manifold of the equilibrium $(z_2, \kappa_2, \gamma_2) = (-1, 0, \gamma)$, is used in the definition of the Evans function in (2.6).*

If $n > 2$, the same discussion as above shows that $z_+(\gamma) = (2 - n) + \mathrm{o}(1)$ so that $\mathcal{E}(0) \neq 0$. For $1 \leq n < 2$, the stability properties of the two equilibria on the z_1-axis are interchanged, and the singular heteroclinic orbit converges to $z_1 = 0$ so that $z_+(\gamma) = \mathrm{o}(1)$ and $\mathcal{E}(0) = 0$. The case $n = 2$ is precisely on the boundary between these two regions characterized by a transcritical bifurcation at $(z_1, \gamma_1, \kappa_1) = 0$. Still, we have $\mathcal{E}(0) = 0$ in this case.

In other words, the heteroclinic orbit from the singular to the rescaling chart, which arises as the limit of the stable subspace of (2.2) as $\gamma \to 0$, always comes from the solution of (2.2) that decays fastest. For $1 \leq n \leq 2$, the fastest decaying solution is the constant solution, while it is $u(r) = r^{2-n}$ for $n > 2$. On the other hand, the only solution that satisfies the boundary condition at $r = 0$ is the constant solution. This explains again why the Evans function vanishes at $\gamma = 0$ for $1 \leq n \leq 2$ but not for $n > 2$. It is perhaps worthwhile to mention that the asymptotic system, i.e. (2.2) with $r = \infty$, is always the same independently of n.

The entire picture is robust under small perturbations of the form $\varepsilon[\mathrm{o}(1/r)u_r + \mathrm{o}(1/r^2)u]$. In particular, the singular heteroclinic orbit as well as the equilibria in the two singular subspaces $\kappa_1 = 0$ and $\gamma_2 = 0$ remain unchanged. Stable and unstable manifolds outside of these subspaces become slightly deformed. Therefore, the Evans function $\mathcal{E}$ depends continuously on ε. Since $\mathcal{E}$ is non-zero for $\gamma \geq 0$ and $n > 2$, we conclude that small perturbations of the Laplacian cannot create positive eigenvalues, a result which has, of course, been known for a long time [15]. For $1 \leq n \leq 2$, small perturbations may create a small positive eigenvalue $\lambda(\varepsilon)$. Expansions for this eigenvalue $\lambda(\varepsilon)$ can be derived using the methods outlined in Section 3.5.

3 The Evans function for contact defects

3.1 The reduction near contact defects

We consider the reaction-diffusion system

$$U_t = DU_{xx} + F(u), \qquad x \in \mathbb{R}, \tag{3.1}$$

and assume that there exists a family of wave-train solutions $U_{\rm wt}(kx - \omega_{\rm nl}(k)t; k)$ for wavenumbers k close to $k_* \neq 0$ whose dispersion relation $\omega_{\rm nl}(k)$ is genuinely nonlinear so that $\omega''_{\rm nl}(k_*) \neq 0$. Recall that the group velocity is defined by $c_{\rm g} = \omega'_{\rm nl}(k)$. We are interested in contact defects which are solutions of the form $U(x,t) = U_{\rm d}(x - c_{\rm g}t, \omega_{\rm d}t)$ where $U_{\rm d}(\xi,\tau)$ is 2π-periodic in τ with $\omega_{\rm d} = \omega_{\rm nl}(k_*) - c_{\rm g}k_* \neq 0$ and

$$|U_*(\xi,\cdot) - U_{\rm wt}(k_*\xi - \theta_\pm(\xi) - \cdot; k_*)|_{H^1(S^1)} + |\partial_\xi(U_*(\xi,\cdot) - U_{\rm wt}(k_*\xi - \theta_\pm(\xi) - \cdot; k_*))|_{L^2(S^1)} \to 0$$

as $\xi \to \pm\infty$ for appropriate phase functions $\theta_\pm(\xi)$ that satisfy $\theta'_\pm(\xi) \to 0$ as $\xi \to \pm\infty$. Using the co-moving frame $\xi = x - c_{\rm g}t$ and the rescaled time $\tau = \omega_{\rm d}t$, defects can be obtained as solutions to the modulated-wave equation

$$\begin{aligned} U_\xi &= V \\ V_\xi &= -D^{-1}[-\omega_{\rm d}\partial_\tau U + c_{\rm g}V + F(U)] \end{aligned} \tag{3.2}$$

on $Y = H^{1/2}(S^1) \times L^2(S^1)$ with 2π-periodic boundary conditions in τ. Note that we have the S^1-shift invariance $(U,V)(\tau) \mapsto (U,V)(\tau+\theta)$ of (3.2) on Y. The wave trains

$$U_{\rm wt}(k_*x - \omega_{\rm nl}(k_*)t; k_*) = U_{\rm wt}(k_*\xi - \tau; k_*)$$

correspond to $2\pi/k_*$-periodic solutions of (3.2). Introducing the co-rotating frame $\vartheta = k_*\xi - \tau$, we obtain

$$\begin{aligned} U_\xi &= k_*\partial_\vartheta U + V \\ V_\xi &= k_*\partial_\vartheta V - D^{-1}[\omega_{\rm d}\partial_\vartheta U + c_{\rm g}V + F(U)]. \end{aligned} \tag{3.3}$$

In these co-rotating coordinates, the wave trains correspond to circles of equilibria. The contact defect can be viewed as a homoclinic orbit to this circle of equilibria induced by the wave trains.

We assume that the wave trains are asymptotically stable as solutions to (3.1) posed on the space of L^2-functions with period $2\pi/k_*$. In particular, the critical spectrum of the linearization about a wave train is given by an algebraically simple eigenvalue at $\lambda = 0$ which is caused by translation invariance. We also assume that the right-most spectrum of the linearization, considered in $L^2(\mathbb{R})$, in a frame moving with the speed $c_{\rm p} = \omega_{\rm nl}(k_*)/k_*$ of the wave trains is given by the linear dispersion curve $\lambda(\nu)$ with $\lambda(0) = 0$ and $\lambda''(0) > 0$, where $\nu \in \mathbb{C}$ is the spatial growth rate of eigenfunctions. We refer to [4] for more details. Since we passed to a frame that moves precisely with the group velocity $\omega'_{\rm nl}(k_*)$ of the wave trains, we can vary the wavenumber without changing,

to first order, the frequency. As a consequence, the derivative of the wave trains with respect to the wavenumber satisfies the linearized equation: this shows that the linearization of (3.3) about the circle of equilibria has a double eigenvalue at zero.

Thus, as shown in [4], we can reduce the dynamics of (3.2) near the circle of equilibria to a two-dimensional center manifold. The reduced equation on the center manifold is

$$\begin{aligned} \theta_\xi &= \kappa \\ \kappa_\xi &= -f(\kappa) \end{aligned} \tag{3.4}$$

where $\theta \in S^1$, $\kappa \in \mathbb{R}$ and

$$f(\kappa) = -\frac{\omega_{\rm nl}''(0)}{\lambda''(0)}\,\kappa^2 + \mathrm{O}(\kappa^3) =: f_2\kappa^2 + \mathrm{O}(\kappa^3).$$

Note that $f_2 \neq 0$ provided $\omega_{\rm nl}'' \neq 0$ which we assumed to be the case.

We remark that contact defects typically converge along the direction of the center manifold. In particular, the wavenumber $\kappa(\xi)$ converges to zero for $\xi \to \infty$, whereas the phase $\theta(\xi)$ diverges logarithmically as mentioned earlier. The nongeneric case of stronger exponential decay towards the asymptotic wave trains is actually far easier to deal with, since the Evans function can be extended using the Gap Lemma [8, 14].

If we allow the temporal frequency ω to vary near $\omega_{\rm d}$ (which amounts to replacing $\omega_{\rm d}$ by ω and k_* by k in (3.3)), then the reduced vector field is given by [4]

$$f(\kappa) = -\frac{1}{\lambda''(0)}\left[\omega_{\rm nl}''(0)\kappa^2 - (\omega - \omega_{\rm d})\right] + \mathrm{O}(\kappa^3).$$

In particular, if we assume that $\omega_{\rm nl}'' > 0$, say, then we find two wave trains for $\omega > \omega_{\rm d}$, and no wave train for $\omega < \omega_{\rm d}$. In the spatial dynamical system (3.3), the circle of equilibria therefore undergoes a saddle-node bifurcation when ω is varied near $\omega_{\rm d}$.

Next, consider the linearized equation

$$\begin{aligned} u_\xi &= [k_* + \theta'(\xi)]\partial_\vartheta u + v \\ v_\xi &= [k_* + \theta'(\xi)]\partial_\vartheta v - D^{-1}[\omega_{\rm d}\partial_\vartheta u + c_{\rm g} v + F'(U_{\rm d})u - \lambda u] \end{aligned} \tag{3.5}$$

in the co-rotating coordinate $\vartheta = k_*\xi + \theta(\xi) - \tau$, where the contact defect $U_{\rm d}$ is determined by the nonlinear problem (3.3). The eigenvalue parameter λ represents temporal Floquet exponents of the linearization of the period map of (3.3) about the contact defect. Since we assumed that there exists a unique dispersion curve $\lambda(\nu)$ that touches the imaginary axis at $\lambda = 0$ with $\lambda''(0) > 0$, the non-autonomous equation (3.5) has an exponential dichotomy both on $\mathbb{R}_+$ and on $\mathbb{R}_-$ for each value of $\lambda \neq 0$ for which $\mathrm{Re}\,\lambda \geq 0$ [20]. In particular, there exist stable and unstable subspaces $E_+^{\rm s}(\lambda)$ and $E_-^{\rm u}(\lambda)$ that consist precisely of all initial data at $\xi = 0$ of solutions to (3.5) that exist and are bounded on $\mathbb{R}^+$ and $\mathbb{R}^-$, respectively. The subspaces $E_-^{\rm u}(\lambda)$ and $E_+^{\rm s}(\lambda)$ depend analytically on λ in the sense that there exist bounded projections onto $E_-^{\rm u}(\lambda)$ and $E_+^{\rm s}(\lambda)$ that are analytic in λ. In addition, the injection map

$$\iota(\lambda): \quad E_-^{\rm u}(\lambda) \times E_+^{\rm s}(\lambda) \longrightarrow Y, \quad (w_-, w_+) \longmapsto w_- + w_+ \tag{3.6}$$

is Fredholm with index zero. The injection $\iota(\lambda)$ has a bounded inverse precisely when λ does not belong to the Floquet point spectrum. The dimension of the kernel of $\iota(\lambda)$ is equal to the geometric multiplicity of λ as a Floquet exponent of the linearized period map. The algebraic multiplicity of λ can be obtained by adding the dimensions of the kernels of the derivatives $\partial_\lambda^n \iota(\lambda)$ for $n \geq 0$. In fact, Jordan chains can be computed directly using Lyapunov-Schmidt reduction on the finite-dimensional kernel of $\iota(\lambda)$. We refer to [20] for proofs and further details of the above statements. Our goal here is to show that $\iota(\lambda)$ can be continued across $\lambda = 0$ and to derive an expansion in the most interesting cases.

Theorem 1 *In the above setting, the function ι can be continued analytically to a sufficiently small neighborhood of $\lambda = 0$ in $\mathbb{C}$ with a cut taken along the negative real axis $\lambda < 0$. The subspaces $E_-^{\mathrm{u}}(\lambda)$ and $E_+^{\mathrm{s}}(\lambda)$ are C^∞-functions of $\sqrt{\lambda}$ and $\sqrt{\lambda}\log\lambda$ in the region $\operatorname{Re}\sqrt{\lambda} \geq 0$. Furthermore, there exists an analytic function $\mathcal{E}_0(\sqrt{\lambda}, \sqrt{\lambda}\log\lambda)$, defined for all λ close to zero except for λ on the negative real axis $\lambda < 0$. Its extension to $\operatorname{Re}\sqrt{\lambda} \geq 0$ is C^∞ in both arguments. Roots λ of $\mathcal{E}(\sqrt{\lambda}, \sqrt{\lambda}\log\lambda)$ defined by $\mathcal{E}(\gamma, \eta) = \gamma\mathcal{E}_0(\gamma, \eta)$ correspond to Floquet exponents of the linearized period map for each λ to the right of the essential spectrum.*

We prove Theorem 1 in Sections 3.2–3.5 and comment on additional properties of the Evans function in Sections 3.6–3.7.

First, note that (3.5) with $\lambda = 0$ has an exponential trichotomy on $\mathbb{R}^+$ and on $\mathbb{R}^-$. In particular, there are subspaces $E_-^{\mathrm{uu}}(\lambda)$ and $E_+^{\mathrm{ss}}(\lambda)$ that are analytic in λ in a neighborhood of $\lambda = 0$ and that contain precisely those initial data that lead to exponentially decaying solutions on $\mathbb{R}^-$ and on $\mathbb{R}^+$, respectively. In addition, there are two-dimensional complements $E_\pm^{\mathrm{c}}(\lambda)$ which, for $\lambda > 0$, decompose into two one-dimensional subspaces $e_\pm^{\mathrm{s}}(\lambda)$ and $e_\pm^{\mathrm{u}}(\lambda)$. We show below that this decomposition can be continued analytically into $\mathbb{C} \setminus \{\lambda < 0\}$ with C^∞-limits on $\lambda < 0$ from both sides $\operatorname{Im}\lambda > 0$ and $\operatorname{Im}\lambda < 0$. The subspaces $E_-^{\mathrm{u}}(\lambda)$ and $E_+^{\mathrm{s}}(\lambda)$ needed in the definition of $\iota(\lambda)$ are then defined as

$$E_-^{\mathrm{u}} = E_-^{\mathrm{uu}} \oplus e_-^{\mathrm{u}}, \qquad E_+^{\mathrm{s}} = E_+^{\mathrm{ss}} \oplus e_+^{\mathrm{s}}.$$

By construction, $\iota(0)$ is then Fredholm with index zero at $\lambda = 0$, and we can find all eigenvalues from the Lyapunov-Schmidt reduced finite-dimensional equation. In particular, eigenvalues correspond to zeros of the determinant $\mathcal{E}$ of the Lyapunov-Schmidt reduced operator on the finite-dimensional kernel. This completes the construction of $\mathcal{E}$ up to the construction of $e_+^{\mathrm{s}}(\lambda)$ and $e_-^{\mathrm{u}}(\lambda)$ on which we shall concentrate now.

To analyse the flow in the complements $E_\pm^{\mathrm{c}}(\lambda)$, we carry out a simultaneous center-manifold reduction of the nonlinear (3.3) and the linear problem (3.5) near the circle of equilibria. We focus on continuing $E_+^{\mathrm{s}}(\lambda) \cap E_+^{\mathrm{c}}(\lambda)$. Note that once we find a splitting close to the asymptotic circle of equilibria, we can continue this splitting in ξ up to $\xi = 0$ by using the linearized evolution in the two-dimensional space $E_+^{\mathrm{c}}(\lambda)$. Thus, it suffices to investigate the dynamics on the center manifold. We observe that, on the center manifold, we recover the nonlinear equation (3.4) and its linearization. The dependence of the linear problem on λ is the same as that of the nonlinear problem on

ω so that we obtain the system

$$\begin{aligned} \kappa_\xi &= -f(\kappa) \\ u_\xi &= v \\ v_\xi &= -f'(\kappa)v + \lambda u + \mathrm{O}(|\lambda|^2(|u| + |v|)), \end{aligned} \tag{3.7}$$

where we set $v = u_\xi$ and possibly rescale the eigenvalue parameter λ by a positive constant. Recall that the nonlinearity satisfies

$$f(\kappa) = \kappa^2 + f_3\kappa^3 + \mathrm{O}(\kappa^4), \tag{3.8}$$

after rescaling κ. Note also that we omitted the equation for the phase θ since it decouples from the other equations due to equivariance with respect to time shifts.

The strategy is now to follow the analysis presented in Section 2 and to check whether the higher-order terms of f can affect the results.

3.2 The blow-up

Introducing the homogeneous coordinates $z = v/u$ in the complex projective space and the Riemann surface parametrization $\lambda = \gamma^2$, we obtain

$$\begin{aligned} \kappa' &= -f(\kappa) \\ z' &= -f'(\kappa)z + \gamma^2 - z^2 + \mathrm{O}(\gamma^4). \end{aligned} \tag{3.9}$$

Note that the above equation agrees to leading order with the equation (2.3) for the 3-dimensional Laplacian. In particular, (3.9) is, to leading order, homogeneous of degree 2. It is therefore natural to introduce the homogeneous blow-up coordinates from Section 2. The first set of coordinates, again referred to as the *singular chart*, is defined via

$$z_1 = \frac{z}{\kappa}, \qquad \gamma_1 = \frac{\gamma}{\kappa}, \qquad \kappa_1 = \kappa,$$

and (3.9) becomes

$$\begin{aligned} z_1' &= \kappa_1 \left[\frac{f(\kappa_1) - f'(\kappa_1)\kappa_1}{\kappa_1^2} z_1 + \gamma_1^2 - z_1^2 + \mathrm{O}(\gamma_1^4)\kappa_1^2 \right] \\ \gamma_1' &= \kappa_1 \left[\frac{f(\kappa_1)}{\kappa_1^2}\gamma_1 \right] \\ \kappa_1' &= \kappa_1 \left[-\frac{f(\kappa_1)}{\kappa_1^2}\kappa_1 \right]. \end{aligned}$$

Rescaling ξ to remove the Euler multiplier κ_1, we get

$$\begin{aligned} \dot{z}_1 &= \frac{f(\kappa_1) - f'(\kappa_1)\kappa_1}{\kappa_1^2} z_1 + \gamma_1^2 - z_1^2 + \mathrm{O}(\gamma_1^4)\kappa_1^2 \\ \dot{\gamma}_1 &= \frac{f(\kappa_1)}{\kappa_1^2}\gamma_1 \\ \dot{\kappa}_1 &= -\frac{f(\kappa_1)}{\kappa_1^2}\kappa_1. \end{aligned} \tag{3.10}$$

It follows from (3.8) that the subspace $\kappa_1 = 0$ is invariant. Note that we recover the dynamics of the radial Laplacian in three dimensions inside that subspace.

The second set of coordinates, referred to as the *rescaling chart*, is defined by

$$z_2 = \frac{z}{\varepsilon_2}, \qquad \kappa_2 = \frac{\kappa}{\varepsilon_2}, \qquad \gamma_2 = \frac{\gamma}{\varepsilon_2}, \qquad |\gamma_2| = 1,$$

where $\gamma_2 = \mathrm{e}^{\mathrm{i}\varphi} \in \mathbb{C}$ and $\varepsilon_2 \geq 0$, which gives

$$\begin{aligned} z_2' &= \varepsilon_2 \left[-\frac{f'(\varepsilon_2\kappa_2)}{\varepsilon_2} z_2 + \gamma_2^2 - z_2^2 + \mathrm{O}(\varepsilon_2^2) \right] \\ \kappa_2' &= \varepsilon_2 \left[-\frac{f(\varepsilon_2\kappa_2)}{\varepsilon_2^2} \right] \\ \varepsilon_2' &= 0. \end{aligned}$$

After rescaling time, we obtain

$$\begin{aligned} \dot{z}_2 &= -\frac{f'(\varepsilon_2\kappa_2)}{\varepsilon_2} z_2 + \gamma_2^2 - z_2^2 + \mathrm{O}(\varepsilon_2^2) \\ \dot{\kappa}_2 &= -\frac{f(\varepsilon_2\kappa_2)}{\varepsilon_2^2} \\ \dot{\varepsilon_2} &= 0. \end{aligned} \tag{3.11}$$

Equation (3.11) has two lines of equilibria given by $(z_2, \kappa_2, \varepsilon_2) = (\pm\gamma_2 + \mathrm{O}(\varepsilon_2^2), 0, \varepsilon_2)$ that are parametrized by $\varepsilon_2 \geq 0$ and that emanate from the singular equilibria in $\varepsilon_2 = 0$. If $\operatorname{Re}\gamma > 0$, the equilibrium at $z_2 = -\gamma_2$ is unstable inside the invariant plane $\kappa_2 = 0$. For fixed values of the parameter ε_2, its stable manifold (alias the part of the center manifold that lies in $\kappa_2 > 0$) corresponds to the stable subspace of (3.7) we are interested in. The same arguments used for the simple three-dimensional Laplacian now show that this subspace can be continued continuously along the positive real axis $\gamma \geq 0$ into the origin. In the remaining part of Section 3, we consider the continuation of this manifold for complex values of γ with $\operatorname{Re}\gamma \geq 0$ and the derivation of an expansion for this subspace. First, we show in Section 3.3 that the stable manifold depends analytically on γ in the rescaling chart. In Section 3.4, we then construct the singular heteroclinic orbit between the rescaling and the singular chart for complex values of γ. Lastly, in Section 3.5, we analyse the transition map near the hyperbolic equilibrium $z_1 = -1$ in the singular chart which allows us to obtain expansions for the stable subspace at a fixed time $\kappa_1 = \delta$.

3.3 Continuing the stable manifold up to the absolute spectrum

Recall that the stable manifold of the equilibrium $z_2 = \gamma_2$ corresponds to the stable subspace of (3.7) whenever $\operatorname{Re}\gamma_2 > 0$. We show that we can continue this stable manifold into $\operatorname{Re}\gamma_2 \geq 0$ for $\varepsilon_2 \geq 0$ close to zero. We denote by $z_2^* = z_2^*(\gamma_2, \varepsilon_2)$ the equilibrium of (3.11) given by $z_2^* = -\gamma_2 + \mathrm{O}(\varepsilon_2^2)$. Introducing the new variable $\tilde{z}_2$ via $z_2 = z_2^* + \tilde{z}_2 - \kappa_2$ results in the equation

$$\begin{aligned} \dot{\tilde{z}}_2 &= 2\gamma_2\tilde{z}_2 + R(\tilde{z}_2, \kappa_2, \varepsilon_2, \gamma_2) \\ \dot{\kappa}_2 &= -\frac{f(\varepsilon_2\kappa_2)}{\varepsilon_2^2} \\ \dot{\varepsilon_2} &= 0 \end{aligned} \tag{3.12}$$

for the variable $\tilde{z}_2$, where

$$R(\tilde{z}_2, \kappa_2, \varepsilon_2, \gamma_2) = \mathrm{O}((|\kappa_2| + |\tilde{z}_2|)^2).$$

The imaginary axis $\operatorname{Re}\gamma_2 = 0$ corresponds to $\lambda < 0$ which in turn corresponds to the absolute spectrum of the asymptotic wave trains [19], where the eigenvalues of the asymptotic equation have equal real part. Indeed, the equation is real for $\operatorname{Re}\gamma = 0$, so that the eigenvalues in E^{c} are complex conjugates of each other. This shows that the absolute spectrum is indeed located on the negative real axis $\lambda < 0$, and that the linearization at $\tilde{z}_2 = 0$ in the first equation of (3.12) has neutral eigenvalues exactly when $\operatorname{Re}\gamma_2 = 0$ (taking the higher-order terms R into account).

The stable manifold of $(\tilde{z}_2, \kappa_2) = 0$ can be constructed by the usual fixed-point argument. Bounded solutions satisfy the integral equation

$$z(x) = \int_{\infty}^{x} \mathrm{e}^{2\gamma_2(x-y)} R(z(y), \kappa_2(y;\varepsilon_2), \varepsilon_2, \gamma_2)\,\mathrm{d}y, \tag{3.13}$$

where $\kappa_2(y;\varepsilon_2)$ is the solution of the second equation in (3.12). We view (3.13) as a fixed-point equation in the subspace $X = BC^0_1([\ell,\infty),\mathbb{C})$ of those bounded, continuous functions for which $\|z\|_X < \infty$ where

$$\|z\|_X = \sup_{x\geq\ell}(1+|x|)|z(x)|.$$

It is straightforward to verify that the right-hand side of (3.13) defines a contraction, uniformly in $\operatorname{Re}\gamma_2 \geq 0$, in a neighborhood of the origin in X provided $\ell \gg 1$ is sufficiently large. The unique fixed point is analytic in γ for $\operatorname{Re}\gamma_2 > 0$ with a C^∞-limit on the imaginary axis.

3.4 The singular heteroclinic orbit between the singular and the rescaling chart

Consider equation (3.11) with $\varepsilon_2 = 0$:

$$\begin{aligned} \dot{z}_2 &= \gamma_2^2 - 2\kappa_2 z_2 - z_2^2 \\ \dot{\kappa}_2 &= -\kappa_2^2. \end{aligned}$$

If we set $\gamma_2 = \mathrm{e}^{\mathrm{i}\varphi}$ where $\arg\varphi \in [-\pi/2, \pi/2]$, then the stable manifold of the equilibrium $(z_2, \kappa_2) = (-\gamma_2, 0)$ is parametrized by $z_2 = -\mathrm{e}^{\mathrm{i}\varphi} + \mathrm{O}(\kappa_2)$ for small $\kappa_2 > 0$. The point $\kappa_2 = \delta$ on this manifold corresponds in the singular chart to

$$z_1 = \frac{z_2}{\kappa_2} = -\frac{\mathrm{e}^{\mathrm{i}\varphi}}{\delta} + \mathrm{O}(|\delta|), \qquad \gamma_1 = \frac{\gamma_2}{\kappa_2} = \frac{\mathrm{e}^{\mathrm{i}\varphi}}{\delta}, \qquad \kappa_1 = 0 \tag{3.14}$$

since $\kappa_1\gamma_1 = \gamma = \varepsilon_2\mathrm{e}^{\mathrm{i}\varphi}$. We have to consider the backward trajectory with this initial condition for the system

$$\begin{aligned} \dot{z}_1 &= \gamma_1^2 - z_1 - z_1^2 \\ \dot{\gamma}_1 &= \gamma_1. \end{aligned}$$

We change variables according to $Z_1 = z_1 e^{-i\varphi}$ and $\Gamma_1 = \gamma_1 e^{-i\varphi}$ so that $Z_1(0) < 0$ and $\Gamma_1(0) > 0$. In the new variables, the equation reads

$$\begin{aligned} \dot{Z}_1 &= (\Gamma_1^2 - Z_1^2)e^{i\varphi} - Z_1 \\ \dot{\Gamma}_1 &= \Gamma_1. \end{aligned} \tag{3.15}$$

Since $\operatorname{Re} \dot{Z}_1 > 0$ whenever $\operatorname{Re} Z_1 = 0$, we can conclude that $\operatorname{Re} Z_1 < 0$ for all negative times. Since $\Gamma_1 \to 0$ converges to zero exponentially in backward time, Z_1 converges in backward time to the equilibrium $Z_1 = -e^{i\varphi}$ that attracts, in backward time, all solutions of (3.15) in $\operatorname{Re} Z_1 < 0$. Since this equilibrium corresponds to $z_1 = -1$, the desired heteroclinic connection exists.

Let Σ_{in} denote the section $|z_1 + 1| = \delta$ in the singular chart. If we choose $\delta > 0$ sufficiently small, the heteroclinic connection that we found above intersects the section Σ_{in} at a point

$$(z_1, \gamma_1, \kappa_1) = (-1 + z_1^*, \gamma_1^*, 0)$$

where $\gamma_1^* \neq 0$ and $|z_1^*| = \delta$.

Next, we discuss equation (3.11) for small $\varepsilon_2 > 0$. On account of the results in Section 3.3, the stable manifold of the equilibrium near $(z_2, \kappa_2) = (-\gamma_2, 0)$ is differentiable in ε_2. Furthermore, if we solve (3.11) backward in time with an initial condition on this stable manifold, we stay ε_2-close to the heteroclinic orbit that we discussed above. Thus, the intersection of the solution near the heteroclinic orbit with the section Σ_{in} is given by

$$(z_1, \gamma_1, \kappa_1) = (z_{\text{in}}, \gamma_{\text{in}}, \kappa_{\text{in}}) = (-1 + z_1^* + \mathrm{O}(|\varepsilon_2|), \gamma_1^* + \mathrm{O}(|\varepsilon_2|), \varepsilon_2 e^{i\varphi}/\gamma_1^* + \mathrm{O}(|\varepsilon_2|^2)) \tag{3.16}$$

since we have $\kappa_1 \gamma_1 = \gamma = \varepsilon_2 e^{i\varphi}$.

3.5 Logarithmic expansions and the Dulac map

To get expansions for the location of the stable manifold at "time" $\kappa_1 = \delta$ with $\delta > 0$ fixed, we need to analyse the transition map near the equilibrium $(z_1, \gamma_1, \kappa_1) = (-1, 0, 0)$ in the singular chart. Upon introducing the variable $\tilde{z}_1$ defined by $z_1 = -1 + \tilde{z}_1$, using the expansion (3.8)

$$f(\kappa) = \kappa^2 + f_3 \kappa^3 + \mathrm{O}(|\kappa|^4)$$

for f, and rescaling time, equation (3.10) becomes

$$\begin{aligned} \dot{\tilde{z}}_1 &= \tilde{z}_1 + 2f_3\kappa_1 - 3f_3\kappa_1\tilde{z}_1 - f_3\kappa_1\gamma_1^2 + \gamma_1^2 - \tilde{z}_1^2 + f_3\kappa_1\tilde{z}_1^2 + \mathrm{O}(|\kappa_1|^2) + \mathrm{O}(|\kappa_1|^2|\tilde{z}_1|) + \mathrm{O}(4) \\ \dot{\gamma}_1 &= \gamma_1 \\ \dot{\kappa}_1 &= -\kappa_1 \end{aligned} \tag{3.17}$$

where $\mathrm{O}(4) = \mathrm{O}((|\tilde{z}_1| + |\gamma_1| + |\kappa_1|)^4)$. Next, we put (3.17) into normal form. Note that the resonant nonlinear terms that we cannot remove by near-identity polynomial coordinate changes are precisely the monomials of the form

$$|\kappa_1\gamma_1|^k\tilde{z}_1, \qquad |\kappa_1\gamma_1|^k\gamma_1, \qquad |\kappa_1\tilde{z}_1|^k\tilde{z}_1, \qquad |\kappa_1\tilde{z}_1|^k\gamma_1$$

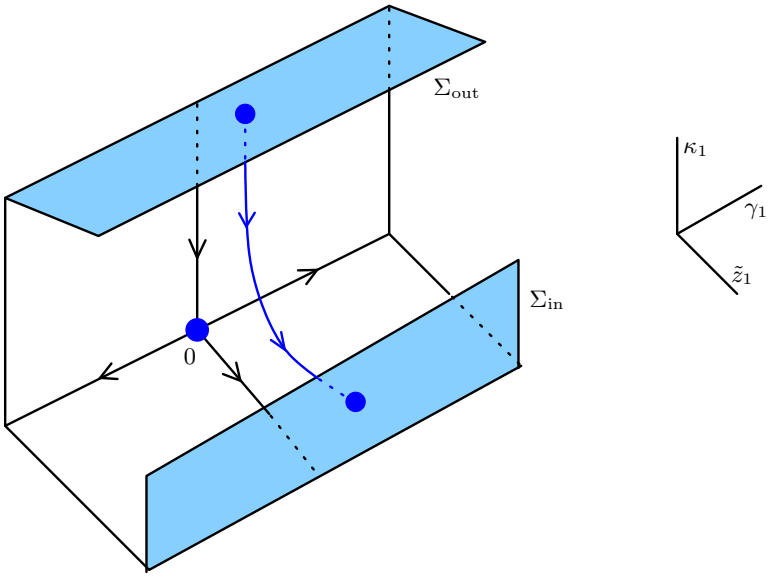

Figure 6: *The Dulac map near $\tilde{z}_1 = 0$, which corresponds to $z_1 = -1$, with sections Σ^{in} and Σ^{out}.*

where $k \in \mathbb{N}$. First, the coordinate change $\tilde{z}_1 \mapsto \tilde{z}_1 + a\kappa_1^2$ for an appropriate $a \in \mathbb{R}$ replaces the $\mathrm{O}(|\kappa_1|^2)$ in (3.17) by $\mathrm{O}(|\kappa_1|^3)$ without changing the other cubic terms. Afterwards, the transformation

$$\tilde{z}_1 \longmapsto \tilde{z}_1 + \gamma^2 - \tilde{z}_1^2 + f_3\kappa_1\tilde{z}_1 \tag{3.18}$$

puts (3.17) into the preliminary normal form

$$\begin{aligned} \dot{\tilde{z}}_1 &= \tilde{z}_1 - 2f_3\kappa_1\gamma_1^2 + \text{non-resonant cubic terms} + \mathrm{O}(4) \\ \dot{\gamma}_1 &= \gamma_1 \\ \dot{\kappa}_1 &= -\kappa_1. \end{aligned} \tag{3.19}$$

Next, we invoke the Sternberg-Chen theorem [3] which shows that an appropriate C^∞-coordinate transformation will put (3.19) exactly into normal form:

$$\begin{aligned} \dot{\tilde{z}}_1 &= \tilde{z}_1(1 + \Phi_1(\tilde{z}_1\kappa_1, \gamma)) - 2f_3\kappa_1\gamma_1^2 + \gamma_1\Phi_2(\gamma) \\ \dot{\gamma}_1 &= \gamma_1 \\ \dot{\kappa}_1 &= -\kappa_1 \end{aligned} \tag{3.20}$$

where Φ_1 and Φ_2 are C^∞-functions that vanish together with their first derivatives at zero, and where we used that $\kappa_1\gamma_1 = \gamma$. Note that the coefficient of the cubic resonant term is zero if, and only if, the cubic coefficient of the nonlinearity f is zero, i.e. if, and only if, the expansion of κ in terms of $1/x$ does not have a quadratic term $1/x^2$.

We then define two sections as follows. The first section Σ^{out} is given by $\kappa_1 = \delta$ and $|\tilde{z}_1|, |\gamma_1| \leq \delta$, while the second section Σ^{in} is defined via $|\tilde{z}_1| = \delta$ and $|\kappa_1|, |\gamma_1| \leq \delta$. We refer to Figure 6 for an illustration and remark that the notation with indices "in" and "out" refers to entering and

leaving a neighborhood of the equilibrium in *backward* time. Note that we can assume that the sections Σ^{out} and Σ^{in} are contained in the image of the above transformation of (3.10) into normal form. We are interested in the local Poincaré map from Σ^{in} to Σ^{out} that is obtained by following trajectories from Σ^{in} backward in time until they first hit Σ^{out} (see again Figure 6).

In fact, we need to calculate the image under the Poincaré map of the initial condition given in (3.16) that corresponds to the continuation of the stable subspace of (3.7). Thus, after applying the coordinate transformations of the z_1 and $\tilde{z}_1$ variables to (3.16), we get the initial data

$$(\tilde{z}_1, \gamma_1, \kappa_1)(0) = (\tilde{z}_{\text{in}}, \gamma_{\text{in}}, \kappa_{\text{in}}) = (\tilde{z}_1^* + \mathrm{O}(|\gamma|), \gamma_1^* + \mathrm{O}(|\gamma|), \gamma/\gamma_1^* + \mathrm{O}(|\gamma|^2)) \tag{3.21}$$

where $\tilde{z}_1^*$ has a certain value that we will calculate in Section 3.7, whereas γ_1^* is as in (3.16) since we never transformed the (γ_1, κ_1) variables. We are interested in computing

$$(\tilde{z}_1, \gamma_1, \kappa_1)(T) = (\tilde{z}_{\text{out}}, \gamma_{\text{out}}, \delta)$$

where T is the time needed to pass from Σ_{in} to Σ_{out} in time (in particular, we have $T < 0$). Using the explicit form of the equation for κ_1, we see that $T = \log(\kappa_{\text{in}}/\delta)$. Recall also that $\kappa_1\gamma_1 = \kappa_1(0)\gamma_1(0) = \gamma$ is independent of time. We introduce the new variable $\zeta_1 = \tilde{z}_1\kappa_1$ which then satisfies the equation

$$\frac{\mathrm{d}\zeta_1}{\mathrm{d}t} = \zeta_1\Phi_1(\zeta_1, \gamma) - 2f_3\gamma^2 + \gamma\Phi_2(\gamma), \qquad \zeta(0) = \tilde{z}_{\text{in}}\kappa_{\text{in}}, \qquad \zeta(T) = \tilde{z}_{\text{out}}.$$

Rescaling space $\tilde{\zeta}_1 = \zeta_1/\kappa_{\text{in}}$ and time $\tau = \kappa_{\text{in}}t$, we obtain the equation

$$\frac{\mathrm{d}\tilde{\zeta}_1}{\mathrm{d}\tau} = \frac{\tilde{\zeta}_1\Phi_1(\kappa_{\text{in}}\tilde{\zeta}_1, \gamma)}{\kappa_{\text{in}}} - \frac{2f_3\gamma^2 - \gamma\Phi_2(\gamma)}{\kappa_{\text{in}}^2}, \qquad \tilde{\zeta}_1(0) = \tilde{z}_{\text{in}}, \qquad \tilde{\zeta}_1(\Theta) = \frac{\tilde{z}_{\text{out}}}{\kappa_{\text{in}}}. \tag{3.22}$$

where $\Theta = \kappa_{\text{in}}\log(\kappa_{\text{in}}/\delta)$. Note that the right-hand side of the ODE for $\tilde{\zeta}_1$ is smooth in a neighborhood of the origin since $(\Phi_1, \Phi_2) = \mathrm{O}(2)$ and $\kappa_{\text{in}} = \mathrm{O}(|\gamma|)$ by (3.21). We denote the associated smooth flow by $\Psi(\tau, \tilde{\zeta}_1(0))$. For the Poincaré map, we then have the explicit expression

$$\tilde{z}_{\text{out}} = \kappa_{\text{in}}\tilde{\zeta}_1(\Theta) = \kappa_{\text{in}}\Psi(\kappa_{\text{in}}\log(\kappa_{\text{in}}/\delta), \tilde{z}_{\text{in}}).$$

In particular, $\tilde{z}_{\text{out}}$ is a smooth function of the variables κ_{in}, $\kappa_{\text{in}}\log\kappa_{\text{in}}$, $\tilde{z}_{\text{in}}$ and γ_{in}. Since the time of flight $\Theta = \kappa_{\text{in}}\log(\kappa_{\text{in}}/\delta)$ converges to zero for $\kappa_{\text{in}} \to 0$, we can expand the flow in terms of Θ and the vector field (3.22) evaluated at the initial condition, and obtain

$$\begin{aligned}
&\Psi(\kappa_{\text{in}}\log(\kappa_{\text{in}}/\delta), \tilde{z}_{\text{in}}) \\
&\quad = \quad \tilde{z}_{\text{in}} + (\kappa_{\text{in}}\log(\kappa_{\text{in}}/\delta))\left(\frac{\tilde{z}_{\text{in}}\Phi_1(\kappa_{\text{in}}\tilde{z}_{\text{in}}, \gamma)}{\kappa_{\text{in}}} - \frac{2f_3\gamma^2 - \gamma\Phi_2(\gamma)}{\kappa_{\text{in}}^2}\right) + \mathrm{O}(|\kappa_{\text{in}}\log\kappa_{\text{in}}|^2).
\end{aligned}$$

Recall that both $\tilde{z}_{\text{in}}$ and κ_{in} are smooth functions of γ. Using the expression (3.21) for these functions, and writing $\eta = \gamma\log\gamma$, we obtain

$$\tilde{z}_{\text{out}} = \left(\frac{\gamma}{\gamma_1^*} + \mathrm{O}(|\gamma|^2)\right)\left[\tilde{z}_{\text{in}}(\gamma) - \frac{2f_3\eta}{(\gamma_1^*)^3} + \mathrm{O}\left((|\gamma| + |\eta|)^2\right)\right]. \tag{3.23}$$

This shows that the function $\iota(\lambda)$ can be continued to a neighborhood of the branch point $\lambda = 0$ and proves Theorem 1.

3.6 Non-analyticity of the Evans function

We state another consequence of equation (3.23).

Theorem 2 *If we have, in the setting of Section 3.1, that*

- *the contact defects converge algebraically to the asymptotic wave trains (which is the generic case),*
- *the contact defects are reversible (i.e. $c_{\mathrm{g}} = 0$, and the defect is either an even function of x or else invariant under the operation $(x, \tau) \mapsto (-x, \tau + \pi)$), and*
- *the null space of the injection map $\iota(0)$, defined in (3.6), is one-dimensional,*

then the function $\mathcal{E}_0(\gamma, \eta)$ from Theorem 1 satisfies

$$\partial_\eta \mathcal{E}_0(0, 0) \neq 0$$

whenever $f_3 \neq 0$. In particular, the Evans function is not analytic in γ near $\gamma = 0$.

We remark that Theorem 2 implies that the Evans function is not analytic for an open set of systems. Indeed, defects that are close to reversible defects will travel with small non-zero group velocity, while retaining the logarithmic terms in the associated Evans function. We are not aware of a structure in the system that would enforce logarithmic terms to vanish for an open set of wavenumbers.

To prove Theorem 2, we decompose the eigenvalue problem into even and odd eigenfunctions which can be captured by the modified maps

$$\begin{aligned} \iota_{\mathrm{Neu}}(\lambda): &\qquad E_{\mathrm{Neu}} \times E^{\mathrm{s}}_+(\lambda) \longrightarrow Y, \quad (w_-, w_+) \longmapsto w_- + w_+ \\ \iota_{\mathrm{Dir}}(\lambda): &\qquad E_{\mathrm{Dir}} \times E^{\mathrm{s}}_+(\lambda) \longrightarrow Y, \quad (w_-, w_+) \longmapsto w_- + w_+, \end{aligned}$$

where $E_{\mathrm{Neu}} = H^{1/2} \times \{0\}$ and $E_{\mathrm{Dir}} = \{0\} \times L^2$ in $H^{1/2}(S^1) \times L^2(S^1)$. We find two reduced Evans functions $\mathcal{E}_{\mathrm{Neu}}$ and $\mathcal{E}_{\mathrm{Dir}}$ associated with ι_{Neu} and ι_{Dir}, respectively. The product $\mathcal{E} = \mathcal{E}_{\mathrm{Neu}}\mathcal{E}_{\mathrm{Dir}}$ is an Evans function for the full eigenvalue problem. Since $\mathcal{E}_{\mathrm{Dir}}$ does not vanish in $\lambda = 0$, the leading order terms in the expansion for $\mathcal{E}$ are given by $\mathcal{E}_{\mathrm{Neu}}$. Since E_{Neu} does not depend on λ, the Lyapunov-Schmidt reduced equation for $\iota_{\mathrm{Neu}}(\lambda) = 0$ contains precisely the $\sqrt{\lambda}\log\lambda$-terms from the expansion in the far field.

3.7 The derivative of the Evans function at the branch point

Lastly, we prove that $\gamma = 0$ is a simple root of the Evans function for reversible contact defects that satisfy the assumptions stated in Theorem 2. Using (3.23) and the results stated in Section 3.1, it is not difficult to prove that

$$\frac{\mathrm{d}\mathcal{E}_{\mathrm{Neu}}}{\mathrm{d}\gamma}(0) = \frac{\mathrm{d}\tilde{z}_{\mathrm{out}}}{\mathrm{d}\gamma}(0) = \frac{\tilde{z}_{\mathrm{in}}(0)}{\gamma_1^*}$$

possibly up to a non-zero factor. Thus, it suffices to prove that $\tilde{z}_{\rm in}(0) \neq 0$. Recall that this expression originated in (3.21) and (3.16) as the endpoint of the heteroclinic orbit that connects the singular and the rescaling chart. We calculate the heteroclinic orbit in the new chart

$$z_3 = z, \qquad \gamma_3 = \frac{\gamma}{z}, \qquad \kappa_3 = \frac{\kappa}{z}.$$

In this chart, equation (3.9) becomes

$$\begin{aligned}
\dot{z}_3 &= -f'(z_3\kappa_3) + z_3\gamma_3^2 - z_3 + \mathrm{O}(z_3^3\gamma_3^4) \\
\dot{\gamma}_3 &= \frac{f'(z_3\kappa_3)}{z_3}\,\gamma_3 - \gamma_3^3 + \gamma_3 + \mathrm{O}(z_3^2\gamma_3^5) \\
\dot{\kappa}_3 &= \frac{f'(z_3\kappa_3)}{z_3}\,\kappa_3 - \frac{f(z_3\kappa_3)}{z_3^2} - \kappa_3\gamma_3^2 + \kappa_3 + \mathrm{O}(z_3^2\kappa_3\gamma_3^4)
\end{aligned}$$

after rescaling the independent variable to remove the Euler multiplier z. Note that

$$z_3 = z_1\kappa_1 = z_2\gamma_2, \qquad \gamma_3 = \frac{\gamma_1}{z_1} = \frac{1}{z_2}, \qquad \kappa_3 = \frac{1}{z_1} = \frac{\kappa_2}{z_2}.$$

The heteroclinic orbit between the singular and the rescaling chart that we discussed in Section 3.4 lies in $\kappa_1 = \gamma_2 = 0$ which means that it lies in $z_3 = 0$. Upon setting $z_3 = 0$, we obtain the system

$$\begin{aligned}
\dot{\gamma}_3 &= \gamma_3[2\kappa_3 - \gamma_3^2 + 1] \\
\dot{\kappa}_3 &= \kappa_3[\kappa_3 - \gamma_3^2 + 1].
\end{aligned} \tag{3.24}$$

The equilibria that are connected by the heteroclinic orbit transform according to

$$(z_1, \gamma_1) = (-1, 0) \longmapsto (\gamma_3, \kappa_3) = (0, -1), \qquad (z_2, \gamma_2) = (-1, 0) \longmapsto (\gamma_3, \kappa_3) = (-1, 0).$$

In particular, the heteroclinic orbit that we seek lies on the line $\gamma_3 + \kappa_3 = -1$ which is invariant under the flow of (3.24). Expanding near $(\gamma_3, \kappa_3) = (-1, 0)$, we obtain that the endpoint $(z_{\rm in}, \gamma_{\rm in})$ of the heteroclinic orbit that satisfies $|z_{\rm in} + 1| = \delta$ is given by

$$\begin{aligned}
z_{\rm in} &= \frac{1}{\kappa_3} = \frac{1}{-1-\gamma_3} = -1 - \delta \\
\gamma_{\rm in} &= \frac{\gamma_3}{\kappa_3} = \frac{\gamma_3}{-1-\gamma_3} = \delta + \mathrm{O}(\delta^2).
\end{aligned}$$

Upon transforming $(z_{\rm in}, \gamma_{\rm in})$ into $(\tilde{z}_{\rm in}, \gamma_{\rm in})$ using the coordinate changes given in Section 3.5, we finally obtain

$$(\tilde{z}_1^*, \gamma_1^*) := (\tilde{z}_{\rm in}, \gamma_{\rm in}) = (-\delta, \delta) + \mathrm{O}(\delta^2)$$

so that

$$\frac{\tilde{z}_{\rm in}(0)}{\gamma_1^*} = -1 + \mathrm{O}(|\delta|) \neq 0$$

for δ sufficiently small. In summary, we proved the following theorem.

Theorem 3 *Under the assumptions of Theorem 2, we have*

$$\frac{\mathrm{d}}{\mathrm{d}\gamma}\mathcal{E}(\gamma, \gamma\log\gamma)\Big|_{\gamma=0} = \mathcal{E}_0(0,0) \neq 0$$

so that $\gamma = 0$ is a simple root of the C^1-function $\mathcal{E}(\gamma, \gamma\log\gamma)$.

4 Discussion

We conclude this paper by commenting on a number of related issues and by indicating how the technique presented here can be applied to some other open problems.

The role of zeros of the Evans function

A legitimate question is whether zeros of the Evans function at the branch point $\lambda = 0$ play any role at all for the temporal dynamics. One might argue that "embedded eigenvalues", objects studied thoroughly, for instance, in the context of linear Schrödinger operators in L^2-function spaces, should be the relevant object for the asymptotic temporal dynamics. We claim that the extension of the Evans function provides the correct intuition for the temporal asymptotics. Our argument is based on well-known results for the long-time behaviour of solutions to the radial Laplacian that follows from pointwise estimates for the Green's function of the linear heat equation with potentials and drift terms [16]. Consider, for instance, the heat equation

$$u_t = u_{xx}$$

on $\mathbb{R}$. Its Green's function $G(x,t)$ has the asymptotics

$$G(x,t) \sim \frac{a_1}{t^{1/2}} + \frac{a_2}{t^{3/2}} + \dots \tag{4.1}$$

where $a_1 \neq 0$. The associated Evans function can be continued in a smooth fashion to the Riemann surface $\lambda = \gamma^2$ where it has a simple zero at $\gamma = 0$. This zero disappears if we add a localized negative potential $V(x) \leq 0$ to the heat equation. The temporal asymptotics of the Green's function of the resulting equation

$$u_t = u_{xx} + V(x)u$$

is again of the form (4.1) except that the coefficient $a_1 = 0$ vanishes [16, Theorem 5.5] so that the asymptotics changes dramatically. Thus, upon adding an arbitrarily small localized negative potential, solutions decay faster to zero. A similar phenomenon arises in two space dimensions [16, Theorem 5.4], while the asymptotics is unchanged in three space dimensions [16, Theorem 5.3]. This is precisely the behaviour predicted from an analysis of the Evans function: The zero in dimensions $n \leq 2$ disappears under perturbations, whereas $\mathcal{E}(0) \neq 0$ is robust in dimension $n > 2$. A related argument is as follows: Adding a small localized positive potential to the heat equation can create a small unstable eigenvalue, with corresponding small exponential growth of solutions, in dimensions $n \leq 2$ but not in dimensions $n > 2$.

The Kolmogorov-Petrovsky-Piskunov equation and the radial Laplacian in $\mathbb{R}^3$

The asymptotics of the radial Laplacian in $\mathbb{R}^3$ arises also in the Kolmogorov-Petrovsky-Piskunov equation

$$u_t = u_{xx} + u - u^2, \qquad x \in \mathbb{R}.$$

This equation has a unique travelling wave $u_*(x-2t)$ with speed 2 that satisfies $u_*(\xi) \to 1$ as $\xi \to -\infty$ and $u_*(\xi) \to 0$ as $\xi \to \infty$. Gallay [7] derived the temporal decay asymptotics of perturbations $v(\xi,t)$ to u_*. After applying Kirchgässner's [13] Eich transformation $v(t,\xi) = w(t,\xi)u_*'(\xi)$, the linear part of the equation for w becomes the three-dimensional Laplacian in the limit $\xi \to \infty$. Since translations of the profile corresponds to constant functions $w \equiv 1$ that do not lie in the kernel of the three-dimensional Laplacian, it is reasonable to expect that the asymptotics are indeed governed by the same expansion as those for the heat equation in $\mathbb{R}^3$. Gallay [7] derived such an expansion for the solutions to the full nonlinear equation.

Note that zeros of the Evans function for the linearized problem

$$v_{xx} + v - 2u_*v = \lambda v \tag{4.2}$$

can be computed from the analytic extension of the Evans function to the Riemann surface $\lambda = \gamma^2$ that is possible due to the Gap Lemma [8, 14]. At $\lambda = 0$, (4.2) written as a first-order system has a branch point that is caused by a Jordan block of the eigenvalue $\nu = -1$. Since the stable subspace converges to the proper eigenspace of the Jordan block, we see that a zero of the Evans function corresponds to a solution with asymptotic decay e^{-x}. Since the wave decays according to $u_*' \sim \xi \mathrm{e}^{-\xi}$, the derivative u_*' of the wave has a component in the direction of the generalized eigenvector. It does therefore not contribute a zero of the Evans function which is consistent with the much more difficult nonlinear result proved by Gallay.

Beyond the Gap Lemma

With this background, we can interpret our analysis as a continuation of the Evans function onto the boundary of the open domain of validity of the Gap Lemma *at* a branch point. The difficulties that one encounters when trying to extend the Evans function *away* from branch points are somewhat different. We use a simple model to show that blow-up techniques can again be used to extend the Evans function beyond the boundary of validity of the Gap Lemma in an analytic fashion, except for a pole that arises at the boundary. Consider

$$\begin{aligned} \kappa' &= -\kappa \\ V_{\mathrm{u}}' &= (\lambda-1)V_{\mathrm{u}} + a\kappa V_{\mathrm{s}} + \mathrm{O}(\kappa^2)V_{\mathrm{s}} + \mathrm{O}(\kappa)V_{\mathrm{u}} \\ V_{\mathrm{s}}' &= \mathrm{O}(\kappa)V_{\mathrm{s}} + \mathrm{O}(\kappa)V_{\mathrm{u}}, \end{aligned}$$

where V_{s} stands for the coordinate that parametrizes the continuation of the stable subspace beyond the essential spectrum. The idea in [8, 14] is to view the κ-dependent stable subspace as the strong stable manifold of the subspace spanned by V_{s} in $\kappa = 0$. This is possible as long as the eigenvalue in the direction of κ is actually stronger than the eigenvalue in the direction of V_{u}, i.e. for $\lambda > 0$. Continuing the Evans function beyond the Gap Lemma amounts to a continuation of this strong stable manifold into $\lambda \leq 0$. We therefore introduce projective coordinates $z = V_{\mathrm{u}}/V_{\mathrm{s}}$ and obtain

$$\begin{aligned} z' &= -z + \lambda z + a\kappa + \mathrm{O}(2) \\ \kappa' &= -\kappa. \end{aligned}$$

For $\lambda > 0$, the κ-dependent stable subspace corresponds to the strong stable manifold of $z = 0$ which is tangent to the strong stable eigenspace given by $a\kappa = -\lambda z$. To resolve the eigenvalue -1 that has algebraic multiplicity two at $\lambda = 0$, we introduce a second blow-up $\xi = \kappa/z$ and obtain

$$\begin{aligned} \xi' &= -\lambda\xi - a\xi^2 + \mathrm{O}(3) \\ \kappa' &= -\kappa. \end{aligned} \tag{4.3}$$

The stable eigenspace $\xi = -\lambda/a$ can be continued analytically in these coordinates through the transcritical bifurcation in the ξ-equation that occurs at $\lambda = 0$. The resulting strong stable manifold, continued through the bifurcation point, is the continuation of the stable subspace that is necessary for the analytic continuation of the Evans function. In the original projective coordinate, the corresponding subspace is given by $z = \kappa/\xi = -a\kappa/\lambda$ which is analytic except at $\lambda = 0$, where a pole occurs. We mention that similar phenomena have been observed independently in [2, Section 3.3] and [17] in explicit examples.

We note that we assumed that the coefficient a is not zero. If $a = 0$, we expect a pitchfork bifurcation in λ so that $\lambda = \gamma^2$ is again the variable necessary for an analytic description of the subspace through the bifurcation. Note, however, that these bifurcations are determined by coefficients of the non-autonomous terms, in analogy to the resonant terms in the radial Laplacian that were introduced in the singular chart and that describe the influence of the non-autonomous terms.

In passing, we remark that a blow-up similar to (4.3) can also be used to derive the estimate for the Dulac map in Section 3.5 without using the resonant normal form.

Solitary waves with algebraic spatial decay

The method we presented in this paper can be adjusted to more difficult situations. We briefly sketch how the Evans function can be extended for algebraically decaying solitons of the cubic-quintic nonlinear Schrödinger equation

$$\mathrm{i}A_t = A_{xx} - A|A|^2 + \beta A|A|^4. \tag{4.4}$$

We denote by $U(x)$ the positive localized homoclinic solution of the equation

$$U_{xx} - U^3 + \beta U^5 = 0.$$

If we linearize (4.4) about U, we obtain the coupled system

$$\begin{aligned} u_1' &= v_1 \\ v_1' &= 3u_1U^2 - \gamma^2 u_2 \\ u_2' &= v_2 \\ v_2' &= u_2U^2 + \gamma^2 u_1 \\ U' &= V \\ V' &= U^3 \end{aligned}$$

that describes the eigenvalue problem. Note that we omitted the quintic monomials which become irrelevant after the blow-up procedure. For $\gamma^2 > 0$, we parametrize the two-dimensional stable subspace in the form

$$\begin{pmatrix} v_1 \\ v_2 \end{pmatrix} = A \begin{pmatrix} u_1 \\ u_2 \end{pmatrix}, \tag{4.5}$$

where A denotes an appropriate x-dependent 2×2-matrix that replaces the projective coordinate z used in Sections 2 and 3. The result is a Riccati equation for A coupled to the system for (U, V):

$$\begin{aligned} A' &= \begin{pmatrix} 3U^2 & -\gamma^2 \\ \gamma^2 & U^2 \end{pmatrix} - A^2 \\ U' &= V \\ V' &= U^3. \end{aligned} \tag{4.6}$$

For $\gamma > 0$, this equation has the equilibria

$$U = V = 0, \qquad A_\pm = \pm \frac{\gamma}{\sqrt{2}} \begin{pmatrix} 1 & -1 \\ 1 & 1 \end{pmatrix}, \tag{4.7}$$

where A_- corresponds to the stable subspace and A_+ to the unstable subspace. The linearization about A_-, given by the equation

$$A' = -(A_- A + A A_-),$$

has only unstable eigenvalues. Thus, there exists a unique stable manifold of the equilibrium A_- in $U > 0$ which corresponds to the x-dependent stable subspace for eigenvalues to the right of the essential spectrum.

The following procedure is completely analogous to the blow-up procedure of Section 2. We first study the rescaling chart $(A_2, U_2, V_2) = (A/\gamma, U/\gamma, V/\gamma^2)$ in which (4.6) becomes

$$\begin{aligned} \dot{A}_2 &= \begin{pmatrix} 3U_2^2 & -1 \\ 1 & U^2 \end{pmatrix} - A_2^2 \\ \dot{U}_2 &= V_2 \\ \dot{V}_2 &= U_2^3 \end{aligned}$$

after rescaling the independent variable to remove the Euler multiplier γ. In the singular subspace $\gamma = 0$, we continue the stable manifold of the matrix A_-, defined in (4.7), in backward time. Its α-limit set can be found in the singular chart $(A_1, \gamma_1, V_1) = (A/U, \gamma/U, V/U^2)$ in which (4.6) becomes

$$\begin{aligned} \dot{A}_1 &= \begin{pmatrix} 3 & -\gamma_1^2 \\ \gamma_1^2 & 1 \end{pmatrix} - A_1^2 - V_1 A_1 \\ \dot{\gamma}_1 &= -\gamma_1 V_1 \\ \dot{U}_1 &= U_1 V_1 \\ \dot{V}_1 &= 1 - 2V_1^2 \end{aligned}$$

again after rescaling the independent variable to remove the Euler multiplier U. We set $U_1 = 0$, and observe that $\gamma_1 \to 0$ and $V_1 \to -1/\sqrt{2}$ in backward time since $V_1 < 0$. The equation for A_1, with $(\gamma_1, V_1) = (0, -1/\sqrt{2})$ substituted, is given by

$$\dot{A}_1 = \begin{pmatrix} 3 & 0 \\ 0 & 1 \end{pmatrix} - A_1^2 + \frac{1}{\sqrt{2}} A_1,$$

which admits a unique repellor given by

$$A_1^{\mathrm{s}} = -\frac{1}{\sqrt{2}} \begin{pmatrix} 2 & 0 \\ 0 & 1 \end{pmatrix}.$$

We checked numerically that the stable manifold of A_- in the rescaling chart converges in backward time towards A_1^{s}, but did not attempt an analytic proof. Thus, the numerical evidence suggests again that the stable subspace converges, for $\gamma = 0$ and computed in the singular chart, to the stable manifold of A_1^{s} which is given explicitly by $(A_1, \gamma_1, U_1, V_1) = (A_1^{\mathrm{s}}, 0, U_1, -1/\sqrt{2})$ with $U_1 > 0$ arbitrary.

It remains to interpret these results in terms of the original variables. Using $U(x) = \sqrt{2}/x$ as well as (4.5) with $A = UA_1^{\mathrm{s}}$, we see that

$$\begin{pmatrix} u_1' \\ u_2' \end{pmatrix} = \begin{pmatrix} v_1 \\ v_2 \end{pmatrix} = -\frac{U(x)}{\sqrt{2}} \begin{pmatrix} 2 & 0 \\ 0 & 1 \end{pmatrix} \begin{pmatrix} u_1 \\ u_2 \end{pmatrix} = -\frac{1}{x} \begin{pmatrix} 2 & 0 \\ 0 & 1 \end{pmatrix} \begin{pmatrix} u_1 \\ u_2 \end{pmatrix}$$

so that $u_1' = -2u_1/x$ and $u_2' = -u_2/x$ which yields $u_1 = 1/x^2$ and $u_2 = 1/x$. In particular, the x-derivative $\partial_x U(x)$ and the phase derivative $\mathrm{i}U(x)$ lie in the two-dimensional stable subspace and therefore contribute a double root of the Evans function at $\gamma = 0$.

We do not know whether the stable manifold always converges in backward time in the singular chart for critical eigenvalue problems. In principle, it is possible that connections to other equilibria that are not repellors within the singular sphere $U = 0$ (or $\kappa = 0$) exist for exceptional parameter values. Related to this problem is the question whether the singular limit of the stable subspace always consists of solutions with the fastest possible decay. Again, it is possible that solutions in the singular subspace decay slower than solutions outside of this subspace for certain eigenvalue problems.

Acknowledgments B Sandstede was partially supported by the Alfred P Sloan Foundation and by the NSF through grant DMS-0203854. A Scheel was partially supported by the NSF through grant DMS-0203301.

References

[1] J. Alexander, R. Gardner and C.K.R.T. Jones. A topological invariant arising in the stability analysis of traveling waves. *J. Reine Angew. Math.* **410** (1990) 167–212.

[2] O. Baconneau, C.-M. Brauner and J. Hulshof. Multiplicity and stability of travelling wave solutions in a free boundary combustion-radiation problem. Preprint, 2002.

[3] K.-T. Chen. Equivalence and decomposition of vector fields about an elementary critical point. *Amer. J. Math.* **85** (1963) 693–722.

[4] A. Doelman, B. Sandstede, A. Scheel and G. Schneider. The dynamics of modulated wave trains. In preparation.

[5] F. Dumortier. Techniques in the theory of local bifurcations: Blow-up, normal forms, nilpotent bifurcations, singular perturbations. In: "Bifurcations and Periodic Orbits of Vector Fields" (D. Schlomiuk, ed.). Kluwer, Dordrecht, NATO ASI Ser. C **408** (1993) 19–73.

[6] H. Freistühler and P. Szmolyan. Spectral stability of small shock waves. *Arch. Rat. Mech. Analysis* **164** (2002) 287–309.

[7] T. Gallay. Local stability of critical fronts in nonlinear parabolic partial differential equations. *Nonlinearity* **7** (1994) 741–764.

[8] R.A. Gardner and K. Zumbrun. The gap lemma and geometric criteria for instability of viscous shock profiles. *Comm. Pure Appl. Math.* **51** (1998) 797–855.

[9] P. Howard. Pointwise estimates and stability for degenerate viscous shock waves. *J. Reine Angew. Math.* **545** (2002) 19–65.

[10] P. Howard and K. Zumbrun. The Evans function and stability criteria for degenerate viscous shock waves. Preprint, 2002.

[11] T. Kapitula and B. Sandstede. Stability of bright solitary wave solutions to perturbed nonlinear Schrödinger equations. *Physica D* **124** (1998) 58–103.

[12] T. Kapitula, N. Kutz and B. Sandstede. The Evans function for nonlocal equations. Preprint, 2002.

[13] K. Kirchgässner. On the nonlinear dynamics of travelling fronts. *J. Diff. Eqns.* **96** (1992) 256–278.

[14] M. Krupa and P. Szmolyan. Extending slow manifolds near transcritical and pitchfork singularities. *Nonlinearity* **14** (2001) 1473–1491.

[15] L.D. Landau and E.M. Lifschitz. *Quantum Mechanics*. Pergamon Press, New York, 1985.

[16] M. Murata. Large time asymptotics for fundamental solutions of diffusion equations. *Tohoku Math. J.* **37** (1985) 151–195.

[17] D.E. Pelinovsky and V.M. Rothos. Evans function for Lax operators with algebraically decaying potentials. Preprint, 2003.

[18] B. Sandstede. Stability of travelling waves. In "Handbook of Dynamical Systems II" (B. Fiedler, ed.). Elsevier, Amsterdam, (2002) 983–1055.

[19] B. Sandstede and A. Scheel. Absolute and convective instabilities of waves on unbounded and large bounded domains. *Physica D* **145** (2000) 233–277.

[20] B. Sandstede and A. Scheel. On the structure of spectra of modulated travelling waves. *Math. Nachr.* **232** (2001) 39–93.

[21] B. Sandstede and A. Scheel. Defects in oscillatory media—towards a classification. In preparation.

[22] J. Smoller. *Shock Waves and Reaction-Diffusion Equations*. Springer, New York, 1983.

[23] M. Yoneyama, A. Fujii and S. Maeda. Wavelength-doubled spiral fragments in photosensitive monolayers. *J. Amer. Chem. Soc.* **117** (1995) 8188–9191.